Smooth velocity models in reflection tomography for imaging complex geological structures.

P. Lailly, Delphine Sinoquet

Geophys. J Int (1996) **124**, 349–362

IREITEL SECTION

Smooth velocity models in reflection tomography for imaging complex geological structures

P. Lailly and D. Sinoquet

PSI Research Consortium. Institut Français du Pétrole. Heliopare Pau-Pyrenees. 2 Ave Pierre Angot, F-64000 *Pau France*

Accepted 1994 November 24 Received 1994 November 17; in original form 1994 June 1

SUMMARY

Seismic imaging of geological structures with severe lateral velocity variations requires pre-stack depth migration of the seismic data. Such processing requires itself an accurate determination of the distribution of the propagation velocities. Reflection tomography turns out to be quite attractive for this purpose. Furthermore, migration velocity analysis can complete this technique whenever complexity of wave propagation makes the picking of reflection traveltimes very cumbersome, if not impossible. Two different subsurface representations can be used to perform these methods: the blocky model representation and the smooth model representation. In reflection tomography, using blocky models with finite velocity jumps can create shadow zones and the possible non-definition of the forward problem. Smooth models, on the other hand, are created such that they do not have such shadow zones but require specific techniques to integrate *a priori* geological information. Also, use of blocky models for migration brings, in general, artificial dicontinuities to migrated seismic events, thus making almost impossible the interpretation of these events which is the basis of migration velocity analysis. Should we use smooth models, such an interpretation becomes possible. Thus, in spite of some inherent limitations, smooth models are well adapted to run reflection tomography coupled with migration velocity analysis for the imaging of complex geological structures.

Key words: inverse problem, ray tracing, reflection seismology, seismic velocities.

1 INTRODUCTION

In this paper, we are interested in seismic imaging of complex geological structures involving severe lateral velocity variations. A typical example is given in Fig. 1. Fig. 2 shows a seismic section of the same geological structure: the geometries of the different layers are clearly seen, except for times greater than 1.5 s and surface locations ranging between 20 and 22 km, where we are not able to identify significant seismic events. The lateral velocity variations do not allow coherent summation of the seismic events during CMP stacking.

Obtaining a good seismic image of such a structure requires pre-stack depth migration, which itself calls for the accurate determination of the distribution of propagation velocities. In particular, for well-known reasons that we will recall below, the velocity model to be used for pre-stack depth migration must be kinematically consistent with the seismic data. Reflection tomography or traveltime inversion (see e.g. Chiu & Stewart 1987; Bording *et al.* 1987; May & Covey 1983; Harlan 1992) is designed to obtain such a model. As picking of reflection traveltimes can be very cumbersome on complex geological structures, it can be replaced or completed by migration velocity analysis. For the sake of simplicity (and because 3-D migration velocity analysis is not in general use today), we will only consider 2-D problems in this paper.

Migration velocity analysis can, in principle, be implemented in the context of common-shot-record migration (Jacobs *et al.* 1992), but, from a practical point of view, this approach is cumbersome and a common-offset implementation is much more preferable (e.g. Wang *et al.* 1991; Williams, Cowley & Notfors 1992; Williams & Cowley 1993). Common-offset migration gives, for each offset, a migrated image of the recorded reflections: the result is thus a cube of migrated images (Fig. 3). If the velocity model used for migration is correct, the migrated images associated with the different offsets are expected to be identical. The stack of all of these common-offset migrated sections will be referred to as the post-migration stacked section. If the migration velocity model is correct, the events that are added during the post-migration stack are consistent with each other: the events in migration

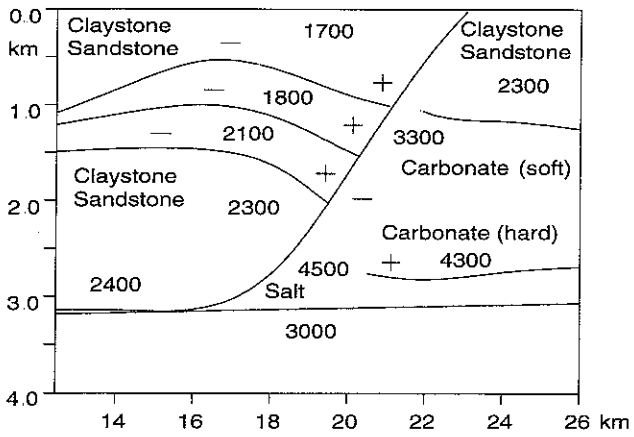

Figure 1. An example of a salt structure at a passive margin. The sediments have slid on a basement that consists of flat layers slightly dipping from the right to the left. This has given rise to a listric fault that juxtaposes materials with very different propagation velocities. The salt may have flowed away, but a salt body may still exist. The + and − signs indicate possible deviations with respect to the indicated velocities.

coherency panels (vertical cuts taken in the cube at a given horizontal location, Fig. 3) are horizontal. If the migration velocity model is erroneous, the events in migration coherency panels are not flat, and incoherent information is summed during the post-migration stack.

The idea behind migration velocity analysis is to use the information contained in the deformation of migrated images from one offset to another to assess the incompatibility between the migration velocity model and the kinematics of seismic data. Yet we can use this information to update the velocity model. Migration velocity analysis basically relies on an interpretation of the cube of migrated images. From such an interpretation, the model can be updated by different techniques, for instance, the ones of van Trier (1990), Stork (1992), and Lailly & Ehinger (1991). The last approach is based on reflection tomography; migration velocity analysis serves to access kinematic information on structures whose complexity makes interpretation of surface seismic sections very difficult. Migration velocity analysis thus yields additional kinematic information that can be processed by reflection tomography.

To run reflection tomography and migration velocity analysis, different subsurface representations can be envisaged. We distinguish two main classes: smooth models and blocky models. The goal of this paper is to examine the role of smooth velocity models in such applications.

2 SUBSURFACE REPRESENTATION FOR REFLECTION TOMOGRAPHY

Reflection tomography is an inverse problem. The forward problem, associated with reflection tomography, is two-point ray tracing between a source and a receiver, which itself relies on a subsurface representation. We will be interested in two different representations of the subsurface.

2.1 The blocky model representation

Blocky models (Lines & Treitel 1985; Chiu & Stewart 1987) use a layer-based representation of the subsurface, each layer being associated with a macrosequence in which the velocity varies gently. Such a representation of the subsurface has a very natural aspect. An example is given in Fig. 4. If x and z denote the horizontal coordinate and the depth, respectively, the mathematical definition of a blocky model requires the definition of:

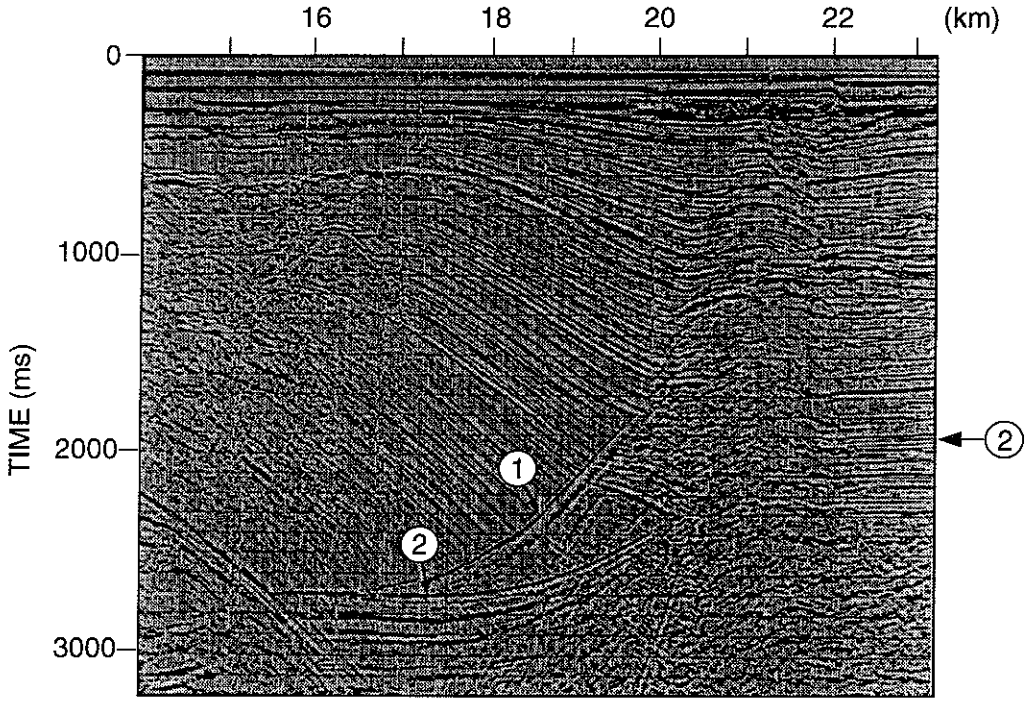

Figure 2. The CMP-stacked section of real data associated with the geological structure in Fig. 1. The arrows indicate the fault (1) and the base of the salt (2).

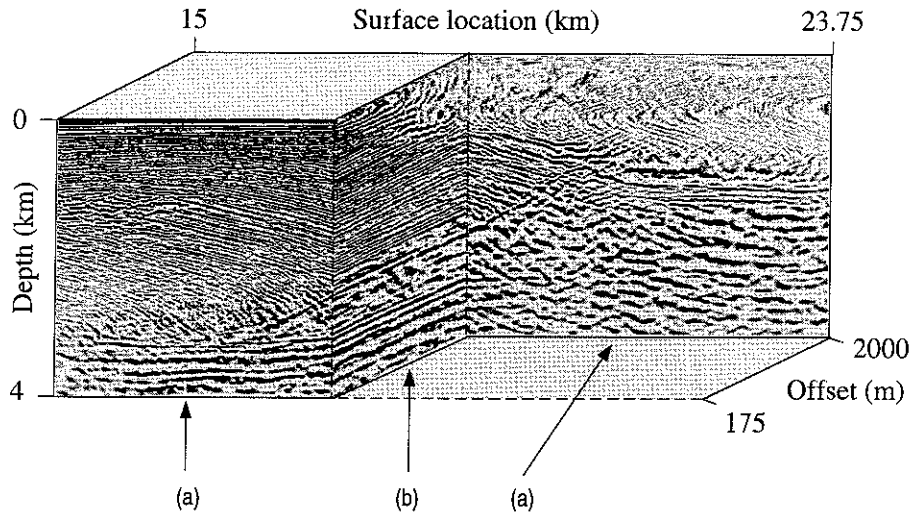

Figure 3. Cube of common-offset migrated images and coherency panels Common-offset migration gives one common-offset migrated image per offset (a) A migration coherency panel (b) is a vertical cut taken in the cube of migrated images for a given horizontal location. Examples of coherency panels are given in Figs 10 and 12

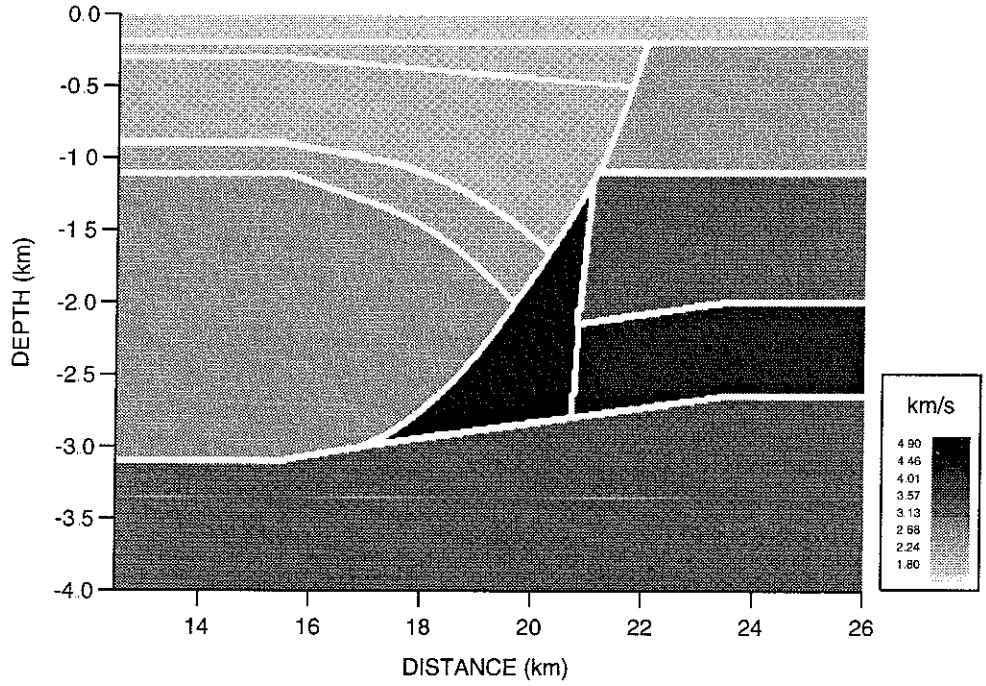

Figure 4. Blocky model associated with the geological structure in Fig. 1. The layer velocities have been chosen as constant, but velocities are generally allowed to vary gentle within each layer

(1) a (slowly varying)[1] velocity distribution $V_i(x, z)$ within each layer i; and

(2) the interfaces separating the different layers For the sake of simplicity, we only consider structures with moderate complexity, thus allowing an explicit representation of the interfaces. They are described by a smooth[1] depth function $Z_j(x)$, the subscript j referring to the interface considered

Finally, for reflection tomography we need to define reflectors: for a blocky model, reflectors are some of the previously defined interfaces.[2] In the following, we denote by $M_{I,J}^{\text{block}}$ the set of blocky models built up of I layers and J interfaces.

2.2 The smooth model representation

In reflection tomography, smooth velocity models with a non-natural character have met with considerable interest (Bishop *et al.* 1985; Bording *et al.* 1987; Harlan 1992; Jacobs *et al.*

[1] We require C^2 regularity to allow the use of paraxial ray techniques, which are very useful for the solution of the two-point ray-tracing problem

[2] Note that not imposing all interfaces to be reflectors increases the generality of the definition of blocky models. Imposing reflectors to be interfaces is not restrictive whenever we allow layers separated by some interfaces to have the same properties

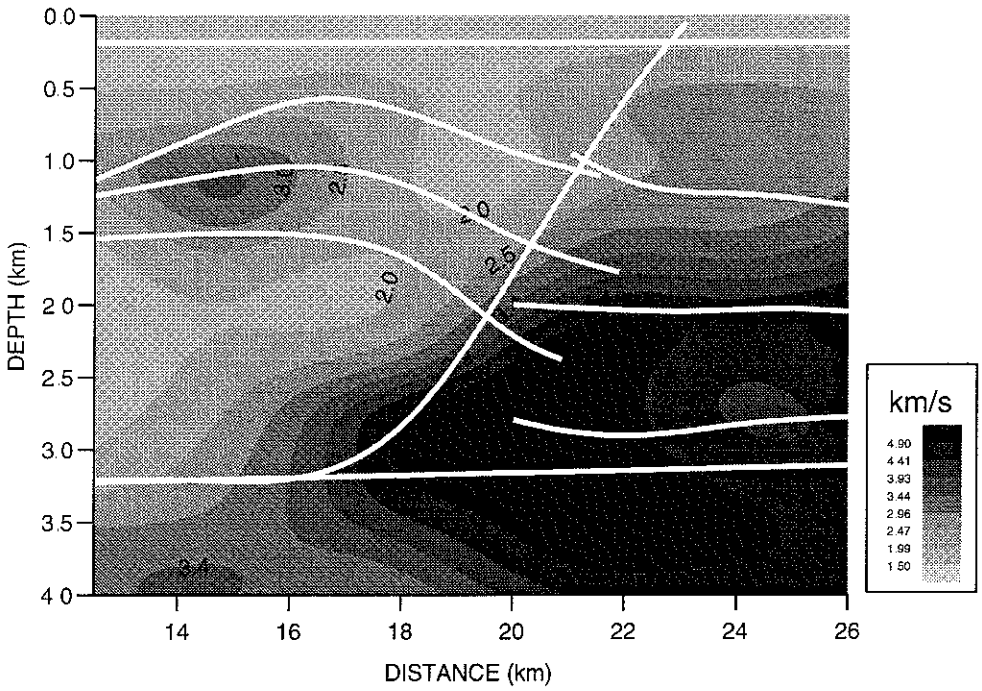

Figure 5. Smooth model associated with the geological structure in Fig. 1. The reflectors are imbedded in the globally defined velocity distribution and are allowed to cross each other. They go from the left to the right of the model. To keep this display clear, we have not drawn the extreme right-hand side of the reflectors to the left of the fault, or the extreme left-hand side of the reflectors to the right of the fault.

1992). In such models, the notion of layers disappears and the velocity distribution is defined globally by a (single) smooth[1] function $V(x, z)$. In smooth models, reflectors are defined by smooth[1] depth functions $Z_j(x)$ imbedded within the velocity distribution $V(x, z)$. An example of such a model is given in Fig. 5. Contrary to blocky models, and for reasons that will be explained later, we allow reflectors in smooth models to cross each other. Thus, a reflector is allowed to cross a fault (Fig. 5). In the following, we denote by M_J^{smooth} the set of smooth models built up of J reflectors.

2.3 The associated forward problems

Having defined the two types of models, we can now define the associated forward problems. We denote by A_j the set of source–receiver pairs (s, r) for which we want to calculate the arrival time of the reflection on reflector j[3].

For a given model $m \in M_{I,J}^{\text{block}}$, two-point ray tracing allows us to compute the arrival times $F_j^{\text{block}}(m)$ of the reflection on reflector $j, j \in J$, for all source–receiver pairs in A_j. Similarly, we denote by $F_j^{\text{smooth}}(m)$ the arrival times of reflection j, where model $m \in M_J^{\text{smooth}}$.

We have thus introduced the forward-modelling operator associated with the reflection tomography problem. Note that the modelling operator F_j^{block} may be undefined for some models in $M_{I,J}^{\text{block}}$: this happens whenever there exists a pair $(s, r) \in A_j$ for which no ray leaving source s can reach receiver r after reflection on reflector j, a common situation, since discontinuous models generate, in general, discontinuous ray families. In contrast, as a consequence of the continuity of ray families for smooth models, the forward modelling operator F_j^{smooth} is, except for rare geometrical situations, defined for all models in F_J^{smooth}[4].

[3] Note that A_j can be empty (case of a blocky model where interface j is not considered as a reflector).

2.4 The associated inverse problems

For the inverse problem, the data are, for a certain number of reflections $j, j \in J$, the multi-offset arrival times T_j^{pick} of each reflection for the different couples (source, receiver) for which this data is available, thus defining the set of measurements A_j. These multi-offset arrival times can be obtained by picking on pre-stack seismic sections. The inverse problem is formulated as a classic least-squares problem. Having defined a norm $\| \ \|_j$ in the space of arrival times associated with reflection j, we want to find the model that best matches this data according to the norms $\| \ \|_j$. We are thus led to the following formulations:

(1) *Blocky model reflection tomography.*
Find $\hat{m}_{\text{block}} \in M_{I,J}^{\text{block}}$ that minimizes

$$C^{\text{block}}(m) = \sum_{j \in J} \| F_j^{\text{block}}(m) - T_j^{\text{pick}} \|_j^2 \qquad (1)$$

(2) *Smooth model reflection tomography*
Find $\hat{m}_{\text{smooth}} \in M_J^{\text{smooth}}$ that minimizes

$$C^{\text{smooth}}(m) = \sum_{j \in J} \| F_j^{\text{smooth}}(m) - T_j^{\text{pick}} \|_j^2 \qquad (2)$$

Delprat-Jannaud & Lailly (1993) show that the above

[4] Difficulties resulting from possible multivalued traveltimes can be overcome either by using a special formulation of reflection tomography (Delprat-Jannaud & Lailly 1995) or by considering the smallest of these traveltimes to define the forward modelling operator. In our paper, we make use of this second strategy.

problems are ill-posed but can be made well-posed by introducing curvature regularization We thus obtain part (3)

(3) *Blocky model reflection tomography with curvature regularization.*

Find $\tilde{m}_{\text{block}} \in M_{I,J}^{\text{block}}$ that minimizes

$$C_{\text{reg}}^{\text{block}}(m) = C^{\text{block}}(m) + \sum_{i \in I} \varepsilon_i^V \int_{D_i} \left[\left(\frac{\partial^2 V_i}{\partial x^2} \right)^2 + \left(\frac{\partial^2 V_i}{\partial z^2} \right)^2 + \left(\frac{\partial^2 V_i}{\partial x \partial z} \right)^2 \right] dx\, dz + \sum_{j \in J} \varepsilon_j^Z \int \left(\frac{\partial^2 Z_j}{\partial x^2} \right)^2 dx, \quad (3)$$

where D_i is the domain associated with layer i, and ε_i^V and ε_j^Z are regularization weights

(4) *Smooth model reflection tomography with curvature regularization.*

Find $\tilde{m}_{\text{smooth}} \in M_J^{\text{smooth}}$ that minimizes

$$C_{\text{reg}}^{\text{smooth}}(m) = C^{\text{smooth}}(m) + \varepsilon^V \int_{D_0} \left[\left(\frac{\partial^2 V}{\partial x^2} \right)^2 + \left(\frac{\partial^2 V}{\partial z^2} \right)^2 + \left(\frac{\partial^2 V}{\partial x \partial z} \right)^2 \right] dx\, dz + \sum_{j \in J} \varepsilon_j^Z \int \left(\frac{\partial^2 Z_j}{\partial x^2} \right)^2 dx, \quad (4)$$

where D_0 is the domain of the overall velocity distribution V, and ε^V and ε_j^Z are again regularization weights.

Minimization of this objective function in reflection tomography is performed classically by an iterative Gauss–Newton algorithm. Note that reflection tomography basically requires the possibility of evaluating how good a model is, by comparing the reflection traveltimes it generates [for all different pairs $(s, r) \in A_j, j \in J$] with the observed times T_j^{pick}. This fundamental requirement is far from fulfiled in blocky-model reflection tomography since the forward modelling operator may be undefined. Reflection tomography is understood as a nonlinear inverse problem, the associated objective function often having several local minima (e.g. Whiting 1991) Non-definition of the forward modelling operator simply increases the chance of being trapped in some local minimum This is not only a theoretical difficulty but, indeed, a practical one For the example in Fig. 4, at some stage of the tomography iterative process, there will not be any ray path joining some sources and receivers lying on either side of the fault This amounts to attributing no importance to the associated picked traveltimes, whereas they contain valuable information when velocity variations in the vicinity of the fault are to be retrieved.

On the other hand, the definition of the forward modelling operators F_j^{smooth} assures that a traveltime exists for each couple $(s, r) \in A_j, j \in J$, so that we expect the objective function $C_{\text{reg}}^{\text{smooth}}$ to be well-behaved. Although we do not claim that local minima do not exist, our many experiments with smooth-model reflection tomography have always provided us with a model that at least matches the data [5]

Application of smooth-model reflection tomography with curvature regularization in our study example produces the result shown in Fig. 6. The fit of calculated and picked traveltimes is very good. However, the model is not satisfying In particular, the distribution of isovelocity lines is rather strange. This should not be surprising and is, in fact, the result of underdetermination Even though smooth-model reflection tomography with curvature regularization is a well-posed problem (in particular, it has a unique solution which is mathematically stable), it is in practice very unstable as a result of: (1) sparse kinematic data (in particular, when we have no traveltime data from the uninterpretable parts of the seismic sections); and (2) the low value given to the regularization weight ε^V

Thus, there exists a very wide variety of smooth models with moderate curvature that match the traveltime data with satisfactory accuracy The solution in Fig. 6 is nothing but an arbitrary representation of all these possible solutions.

Increasing the value of the regularization weight ε^V would improve quantitative stability (Delprat-Jannaud & Lailly 1993), but imposing zero curvature *a priori* (large ε^V) would be contradictory with what we know *a priori* about the velocity (it can vary rapidly, for instance, in the vicinity of the fault) and, in turn, with the kinematics of the seismic data. Instead of this inadequate approach, we have to reduce underdetermination by integrating **relevant** *a priori* geological information

We thus reach the following conclusions.

(1) Blocky-model reflection tomography can lead to a local minimum but offers the advantage of straightforward integration of *a priori* geological information. The solution will meet the *a priori* geological information implicitly contained in the model with the velocity distributions varying gently within a given layer, and with discontinuities at the macrosequence boundaries.

(2) Use of smooth models in reflection tomography assures the convergence to a global minimum. Most importantly, we can expect to take correctly into account the traveltimes associated with rays that travel in the vicinity of, and are most sensitive to velocity variations across, the fault The output of smooth-model reflection tomography with curvature regularization is of limited interest in the case of complex geological structures. The problem is not the use of a smooth model, but the use of global curvature regularization in such situations In other words, use of smooth models for such applications requires the design of an adequate technique for integrating relevant *a priori* geological information into reflection tomography In the next section we re-introduce the concept of layers in smooth models

3 MAKING REFLECTION TOMOGRAPHY WORK WITH SMOOTH MODELS

Integrating *a priori* geological information is essential to reduce the underdetermination inherent in reflection tomography In this section, we examine a variety of geological information and how to integrate it into reflection tomography.

3.1 *A priori* information on the structure of the velocity field

With the exception of turbidites and volcanics, the Earth's subsurface is not chaotic; rather it is governed by processes of

[5] Even though the model is not the one we were looking for, we point out here the very different nature of underdetermination and of convergence towards local minima, i.e., situation in which the computed model does not match the data.

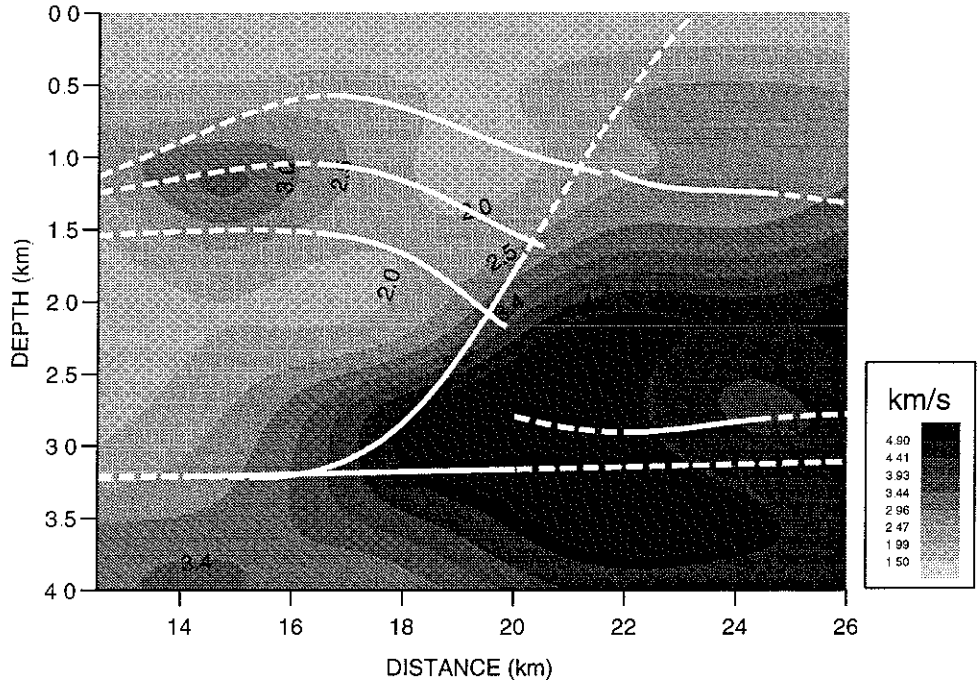

Figure 6. Application of smooth model reflection tomography with curvature regularization. The traveltime data have been obtained by picking seven reflections in the interpretable part of the common-offset seismic sections, associated with the CMP-stacked section of Fig 2. No traveltime data were available for times larger than 1.5 ms and surface locations ranging between approximately 20 and 22 km, because the sections were not interpretable in this area. The parts of the reflectors represented by a dashed line are not illuminated by rays; their geometry is therefore only determined by the integrated zero-curvature *a priori* information. This also indicates those areas that are not crossed by rays, and thus where the velocity is not determined by kinematic data. The RMS traveltime misfit is about 15 ms.

sedimentary deposition and tectonic deformation, such that a given velocity structure results from its geological history. We use two types of geological information on the velocity field: information on the regularity of the velocity and on the anisotropy of regularity due to sedimentation (Sinoquet 1993).

As far as the regularity of the velocity is concerned, we deal only with macroscopic phenomena; very slight velocity variations will not be determined by traveltime inversion. Versteeg (1991) showed that only velocity-field wavelengths of greater than 100 metres are of importance for pre-stack migration. Accordingly, this defines the objective for complex structure tomography. Additionally, geology tells us that velocity is more regular in some places than in others. Fig. 1 shows the possible velocity variations in our study example: we expect large velocity variations in the vicinity of the fault, whereas the velocity should be more regular within the claystone/sandstone formations. Sedimentation results in regular, roughly horizontal deposits, such that velocity varies little along those reflectors that are geological isochrons (Fig. 7). Sedimentation thus gives rise to some anisotropy in the velocity regularity.

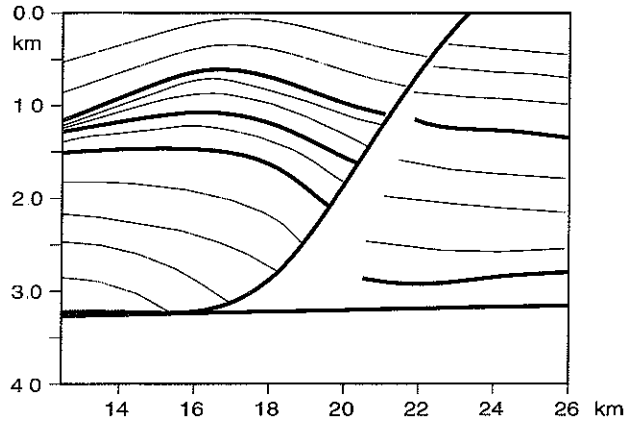

Figure 7. Possible distribution of isovelocity lines according to sedimentation effects for the geological structure in Fig. 1.

To integrate the above-described *a priori* information into reflection tomography, we add penalization terms to the original objective function eq. (2). We obtain

$$C^{\text{smooth}}_{a\ priori}(m) = \underbrace{C^{\text{smooth}}(m)}_{\text{tomography}} + \underbrace{\sum_{j\in J}\int \varepsilon_j^G(m,x)^2[\nabla V(x,Z_j)\cdot \mathbf{t}_j(x)]^2\,dx}_{\text{velocity guide}}$$
$$+ \underbrace{\int_{D_0} \varepsilon^V(m,x,z)^2\left[\left(\frac{\partial^2 V}{\partial x^2}\right)^2+\left(\frac{\partial^2 V}{\partial z^2}\right)^2+\left(\frac{\partial^2 V}{\partial x\partial z}\right)^2\right]dx\,dz}_{\text{velocity regularization}}$$
$$+ \underbrace{\sum_{j\in J}(\varepsilon_j^Z)^2\int\left(\frac{\partial^2 Z_j}{\partial x^2}\right)^2 dx}_{\text{reflector regularization}}, \qquad (5)$$

where ∇V is the gradient of velocity and $\mathbf{t}_j(x)$ is the normalized tangent vector to the reflector j.

The velocity guide term constrains the velocity to vary little along certain reflectors by forcing the gradient of the velocity to be orthogonal to the reflectors: it integrates the *a priori*

information associated with anisotropy of velocity regularity The velocity regularization term controls the velocity variations so as to make them agree with what we expect *a priori* In addition, the velocity regularization term plays an active role in making the isovelocity lines honour the geometry of deposition lines. By imposing gentle variations on the velocity gradient, we keep this gradient approximately orthogonal to the deposition lines that have, within a layer, a geometry similar to the reflectors that surround them. In this way, we can constrain the isovelocity lines and the deposition lines to have similar directions within a whole layer. Finally, the reflector regularization term measures the variations of the slope of the reflectors.

The weighting functions $\varepsilon_j^G(m, x)$, $\varepsilon^V(m, x, z)$, ε_j^Z allow the interpreter to express the uncertainties associated with each piece of information. They are input to our formulation of reflection tomography. They enable us to normalize the functional terms according to their physical meaning. They have been made space- and model-dependent to allow, for instance, large velocity variations in the vicinity of faults whose geometry is to be determined by reflection tomography

The linearized problem associated with the minimization of the objective function $C_{a\ priori}^{\text{smooth}}(m)$ is a well-posed problem: as in Delprat-Jannaud & Lailly (1993), uniqueness and stability of its solution are ensured The model is represented by cubic B-spline functions, adequate to build C^2 functions (Barsky, Bartels & Beatty 1986) The velocity parameters and the interface parameters are thus, respectively, the coefficients of a tensor of B-spline functions defined by an uniform knot grid (x, z), and the coefficients of a B-spine function defined from a uniform sequence of x knots The representation of a smooth velocity model thus requires a large number of parameters. The model shown in Fig 8 is represented by 599, namely 21×25 velocity coefficients and 74 reflector coefficients

3.2 Numerical results

The model in Fig. 8 is the result of tomography integrating the *a priori* information described above To compute it, we have constrained the velocity to vary minimally along the interfaces, except along the fault and the base of the salt. All the interfaces have been regularized by their second derivatives Also, the second derivatives of the velocity have been penalized everywhere, but with different weights according to the region. Indeed, we have defined three zones: the neighbourhood of the fault, where the regularization weight is very low to allow large velocity variations; and the two regions on either side of the fault.

The model in Fig. 8 is satisfactory since: it matches the traveltime data with reasonable accuracy; the velocity varies regularly within each macrosequence and has rapid variations across the fault; and the distribution of isovelocity lines is reasonable

In the region approximately 1 km around the fault, the velocity is poorly determined because of the weak value of the regularization weight in this area Thus, this lack of *a priori* information generates a strange distribution of isovelocity lines around the fault.

The area below the fault (denoted by *A* in Fig 8) is not illuminated by rays at all (as a result of the sparsity of our traveltime data) Consequently, this area is determined only by the integrated *a priori* geological information, in which, however, we have almost no confidence (is there any salt body

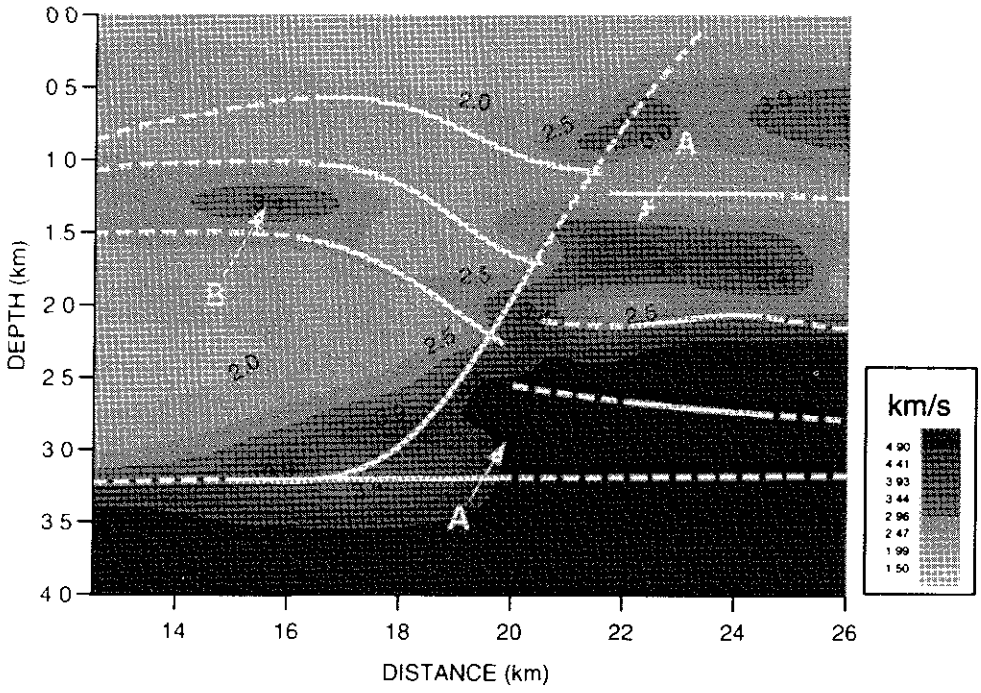

Figure 8. Model obtained by reflection tomography with *a priori* information on the velocity structure with the following weight values: velocity guide $\varepsilon_j^G = 5 \times 10^{-1}$; velocity regularization ε^V in the fault region 10^{-5} on the left- and right-hand sides 10^{-2}; interface regularization $\varepsilon_j^Z = 10^{-1}$ for the interfaces to the right of the fault and 10^{-2} for the others. Compared to the experiment in Fig. 6, an additional reflection has been picked to the right of the fault The RMS traveltime misfit is 16 ms

or do we have a fractured zone with tilted blocks?). In other words, the velocity model is basically undetermined in this area.

Note the velocity anomaly *B* in Fig. 8. It is the result of poor ray coverage, together with limited confidence[6] in the integrated *a priori* geological information, since this area is associated with a fractured zone, as can be seen on the seismic section in Fig. 2.

However, to obtain such a result, the interpreter needs to tune the different weighting functions involved in the definition of our objective function. Neither type of data, traveltimes and *a priori* geological information, is exact, but rather they are only known with limited accuracies. In general, they will be in conflict with each other. The weighting functions in eq (5) have to be correctly tuned so as to obtain a solution that matches the different pieces of information according to the confidence we have in them.

To illustrate the sensitivity to these weights, we show the model in Fig. 9 which was obtained in the same way as the model in Fig. 8, but with different weighting functions; in particular, we increased the weights associated with the velocity regularization and with the velocity guide. This model is very regular on both sides of the fault and presents high velocity variations at the top and the bottom of the fault. The model respects the *a priori* information quite well but does not match traveltimes to the degree of Fig. 8. Such a model is over-regularized. We have not correctly managed our conflicting integrated data. It is the interpreter's job to find a good compromise between the conflicting pieces of information and the subsequent choice of weights.

We can guess *a priori* the order of magnitude of the uncertainty in the different kinds of data. However, an iterative trial-and-error approach turned out to be quite effective to improve those initial guesses for a better calibration of those weights. If the weights guessed *a priori* had led to the model in Fig. 9, we would conclude that, the traveltime match being unacceptable, we should decrease the weights associated with the velocity guide and/or with the velocity curvature. This interpreter-driven approach was effectively used to calibrate iteratively the weights so as to obtain the model in Fig. 8.

3.3 Other kinds of *a priori* geological information

In fact, the result shown in Fig. 8 has been obtained with the help of additional constraints on the model. We constrained the velocity to be equal to 1.5 km s^{-1} and 5 km s^{-1} at the surface and at depth $z = 4$ km, respectively. We also dealt with inequality constraints on the interfaces; for instance, the fault was constrained to be above the base of the salt, and the slope of the interfaces to the right of the fault is constrained to be weak. Additionally, we limited the range of all parameters: the velocity has to be between 1.5 km s^{-1} and 5 km s^{-1} and the interface depths should be between 0 km and 4 km. We thus dealt with 639 inequality constraints and 105 equality constraints. Integrating as much *a priori* information as possible is essential for reducing the underdetermination inherent in reflection tomography. Instead of introducing additional penalization terms in the objective function, we preferred to use constrained optimization algorithms. However, the solution of large-size (several hundreds of parameters, several thousands of data) optimization problems with many constraints of different types can be very difficult. We have used a dedicated algorithm (Glowinski & Tran 1993) based on the augmented Lagrangian technique.

Another kind of information that is especially important for

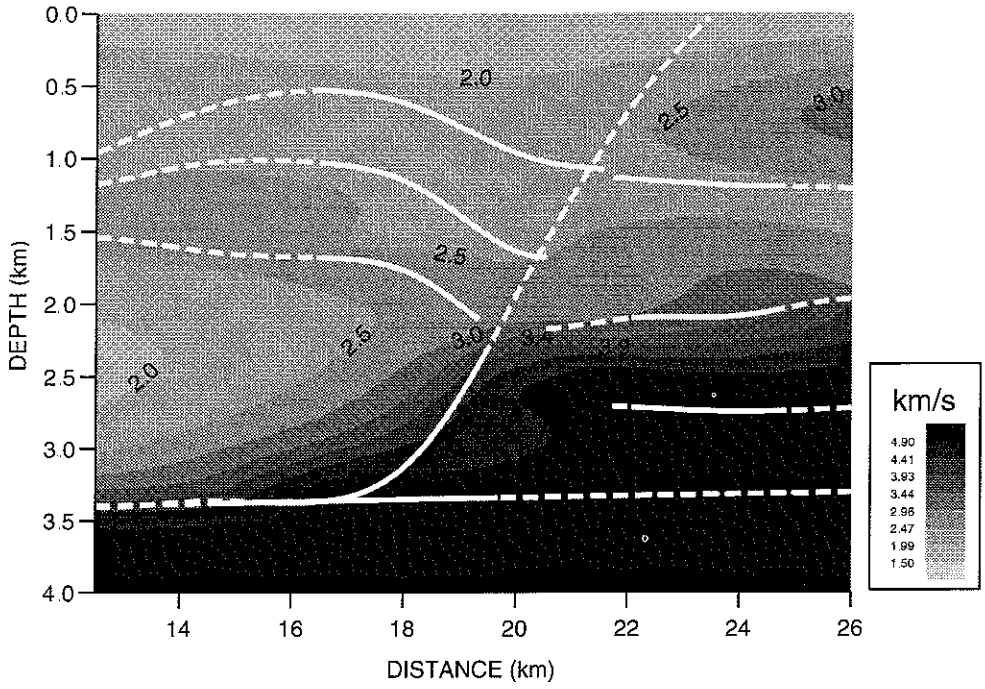

Figure 9. Model obtained by reflection tomography with *a priori* information on velocity structure, but with a different choice of the weight values: velocity guide $\varepsilon_j^G = 5$; velocity regularization ε^V in the fault region 10^{-5}, on the left- and right-hand sides 5×10^{-1}; interface regularization $\varepsilon_j^Z = 10^{-1}$ for the interfaces at the right of the fault and 10^{-2} for the others. The RMS traveltime misfit is 79.2 ms.

[6] See our comments below on the tuning of the weighting functions.

our application is information associated with faults. In order to ensure the definition of the forward modelling operators, it was necessary to allow our reflectors to cross the fault. In fact, we would like the reflectors to end at the fault. In order to meet this requirement, Jannaud & Delprat-Jannaud (1995) have developed a special technique in which they use the location of the impact points of the rays as constraints on the model. However, we have not used this technique to compute the result in Fig. 8: this result shows a moderate extension to the right of reflectors supposed to lie on the left of the fault. This does not seem unreasonable to us since we are processing a 3-D problem on an approximate 2-D dip profile.

3.4 Relations between tomography and migration

Migration is, from a kinematic point of view, the inverse of ray tracing (e.g. Apostoiu-Marin & Ehinger 1994). If we use for migration a velocity model which has been determined by reflection tomography, the migrated images of a picked reflection lie, for each offset, on the reflector determined by tomography.[7] Thus the picked reflections will appear as horizontal events in the migration coherency panels. This can be verified in Fig. 10. Reflection tomography can be understood as a technique to update the velocity model so as to flatten events interpreted in migration coherency panels and to construct coherent summations during the post-migration stack. This leads us to the following definition: a velocity model will be said to be kinematically consistent with some pre-stack picked events if these events appear horizontally aligned in the migration coherency panels when this velocity model is used to perform the migration.

Reflection tomography is thus a means of building a velocity model that is kinematically consistent with some picked events. This might look obvious, but we will see in the next subsection that there are some restrictions to this apparently obvious result.

3.5 Limitations in the use of smooth models in reflection tomography

Use of smooth-model reflection tomography on geological structures with severe lateral variations requires the following conjecture to be true: whatever the velocity discontinuities of a subsurface, it is possible to find a smooth model that matches the traveltimes of seismic data acquired upon this subsurface. We realize that this conjecture does not hold: a subsurface with velocity discontinuities generates discontinuous kinematic events, with respect to both the spatial location of these events and their slopes (e.g. de Bazelaire & Viallix 1988). Attempts at matching such kinematics with a smooth model (that generates continuous events, with respect to both their locations and their slope) would lead to very rapid velocity variations that go beyond the range of applicability of ray tracing. Ray tracing can model the propagation of seismic waves only if the characteristic length of the velocity variations is large with respect to the characteristic wavelength of the seismic waves.

Our interest for smooth models comes from Versteeg (1991) who showed that:

(1) smooth models allow seismic imaging by pre-stack depth migration of very complex geological structures; however, progressive smoothing of the true velocity model gives rise to progressive degradation of the post-migration stacked section;

(2) those smooth models that allow reasonable seismic imaging are those which are approximately kinematically consistent with the pre-stack seismic data; however, the kinematic consistency is progressively degraded when we increase the smoothing of the model.

Thus, using smooth-model reflection tomography, we aim to find an approximately kinematically consistent model. Such a model, used for pre-stack depth migration, yields a migrated image that is only slightly degraded. But, in order to find such a model, we must not go beyond the range of applicability of ray tracing regarding the propagation of seismic waves. We must not allow our smooth velocity models to have rapid variations.

What is the permissable degree of variations for the velocity? In this context it is very helpful to check *a posteriori* that the smooth model that has been computed by reflection tomography is indeed, to a reasonable extent, kinematically consistent with the seismic data.

In the result shown in Fig. 8, we can see that the velocity varies very rapidly for lateral locations ranging between 19 and 20 km. It is thus essential to check the relevance of that part of the model. Migration coherency panels for this interval of lateral locations (Fig. 10, bottom) show a base of salt only slightly deviating from the horizontal. This confirms the good results achieved by smooth-model reflection tomography in computing the result in Fig. 8, and thus confirms the validity of ray tracing for modelling seismic waves in this subsurface area.

The post-migration stacked section (Fig. 11) shows clear seismic events, at least for those parts of the reflectors that have been illuminated by rays (Fig. 8).[8] This is what we expect, since reflection tomography made events kinematically coherent (i.e. produced flat coherency panels) and thus the summation of these events during the post-migration stack is constructive. The lower part of the image, between surface locations 20 and 22 km, is not satisfactory. This is not surprising because the velocity model (Fig. 8) is almost completely undetermined in this area. However, the degradation of the image is progressive when, starting from the right of the section, we enter the undetermined area. This no longer holds if the velocity model used for the migration is blocky, such as the one in Fig. 4. This model has been determined by a kind of manual blocky-model reflection tomography (Delprat-Jannaud *et al.* 1991). Although this model has kinematic qualities (Fig. 12) equivalent to those of the model computed by smooth-model reflection tomography, the post-migration stacked section associated with this blocky model (Fig. 13) shows a very abrupt degradation when horizontal location becomes less than 22 km. This part of the section is composed of many mixed events that make accurate interpretation almost impossible. The reason for this will be given in the next section.

Returning to the smooth-model coherency panels (Fig. 10) we observe some events below the image of the fault that

[7] Whenever reflection tomography has succeeded in matching synthetic and picked traveltimes.

[8] The image is not good in the upper-left corner because the velocity is not well-determined in this area (see the explanations of the velocity anomalies in Fig. 8).

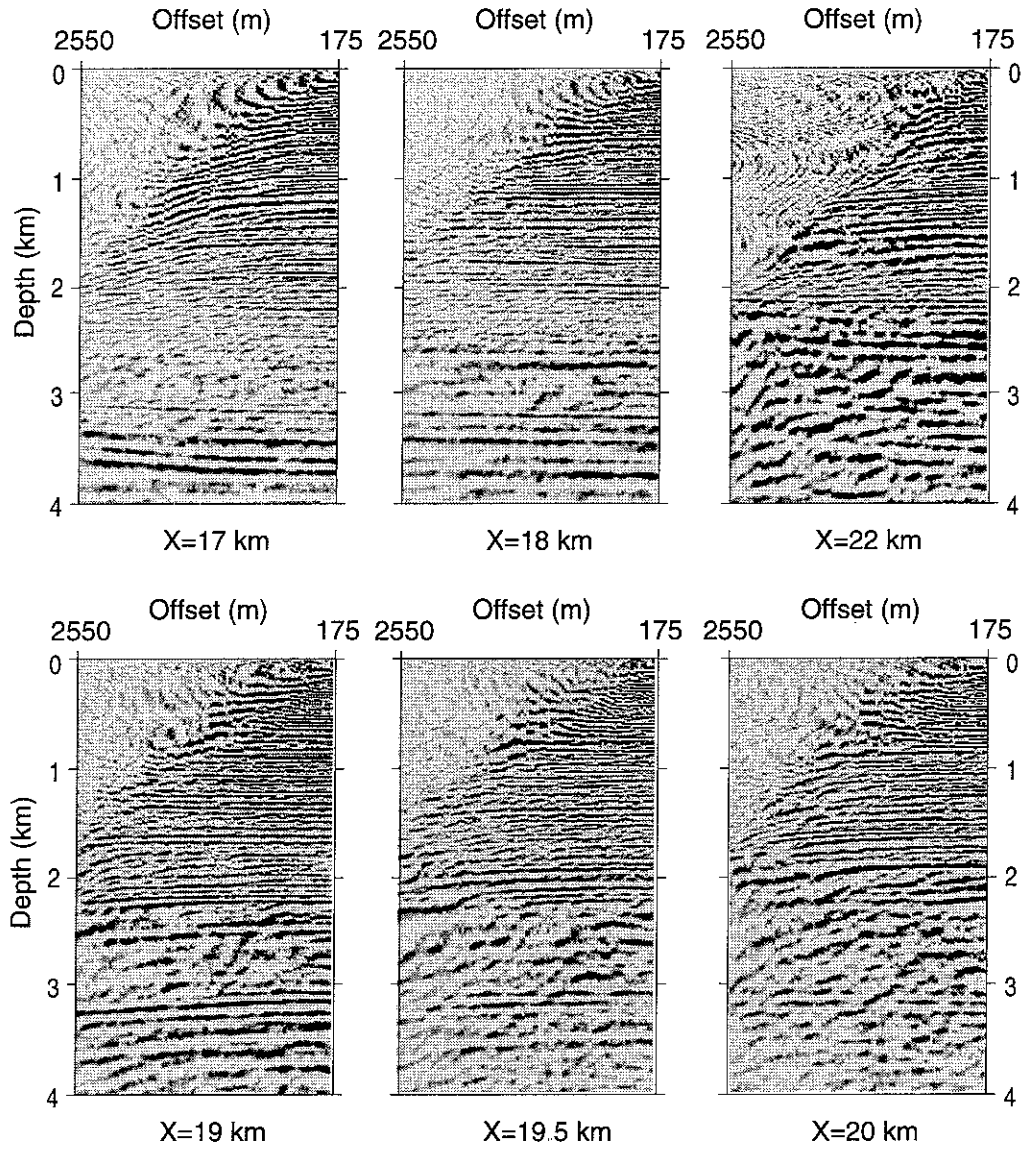

Figure 10. Coherency panels associated with the smooth model in Fig. 8. Top: results for surface locations in the simple part of the subsurface. Flat events illustrate that reflection tomography is an effective technique for constructing a model that is kinematically consistent with the seismic data. For $x = 22$ km, we observe for large offsets some steeply dipping events that are associated with propagation in the complex part of the subsurface. Bottom: results obtained when entering the complex part of the subsurface. Events appear almost flat. This illustrates that reflection tomography has constructed a model approximately kinematically consistent with the seismic data, in spite of the rapid velocity variations. The base of the salt is clearly visible just below depth 3 km. The visible dipping events (for instance, the one clearly visible above the base of the salt for $x = 20$ km) are of prime importance for use in migration velocity analysis.

deviate somewhat from the horizontal. As mentioned before, the goal of migration velocity analysis is to use those deviations and to transform them into additional kinematic data to compute a new and better velocity model.

4 BLOCKY VERSUS SMOOTH MODELS FOR MIGRATION AND MIGRATION VELOCITY ANALYSIS

On complex geological structures, the result of pre-stack depth migration can be very sensitive to the migration algorithm used (e.g. Geoltrain & Brac 1993). In the context of common-offset migration, which seems to be the preferred strategy for migration velocity analysis, Kirchhoff migration has met with considerable interest (e.g. Wang *et al.* 1991; Williams *et al.* 1992). We have to take into account a major difficulty associated with blocky models: Kirchhoff migration makes use of computed traveltimes, and these traveltimes are extremely sensitive to perturbations of the velocity model, especially to perturbations of the geometry of interfaces that separate layers with very different velocities. We must therefore be very careful when specifying a blocky velocity model for Kirchhoff depth migration. In contrast, specifying a smooth model for Kirchhoff depth migration is straightforward. What must not be done is to smooth a carefully determined blocky velocity model and to use this smoothed version as input for Kirchhoff depth

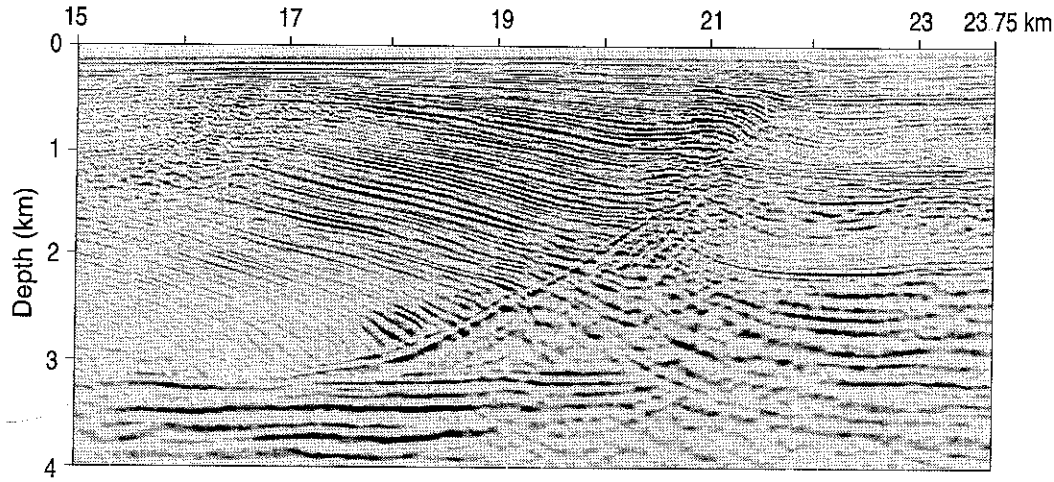

Figure 11. Post-migration stacked section associated with the smooth model in Fig 8

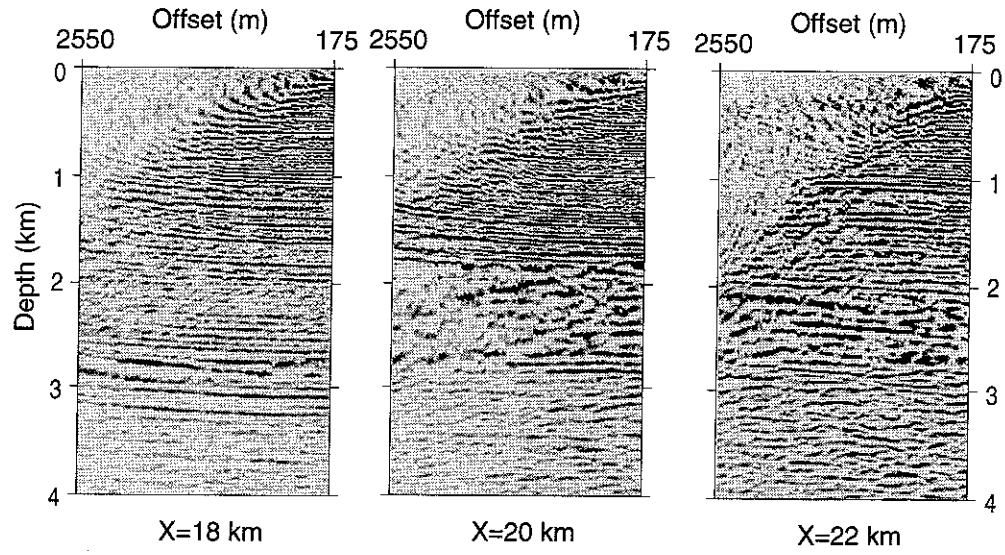

Figure 12. Coherency panels associated with the blocky model in Fig 4. Flat events indicate that the model is approximately kinematically consistent with the seismic data

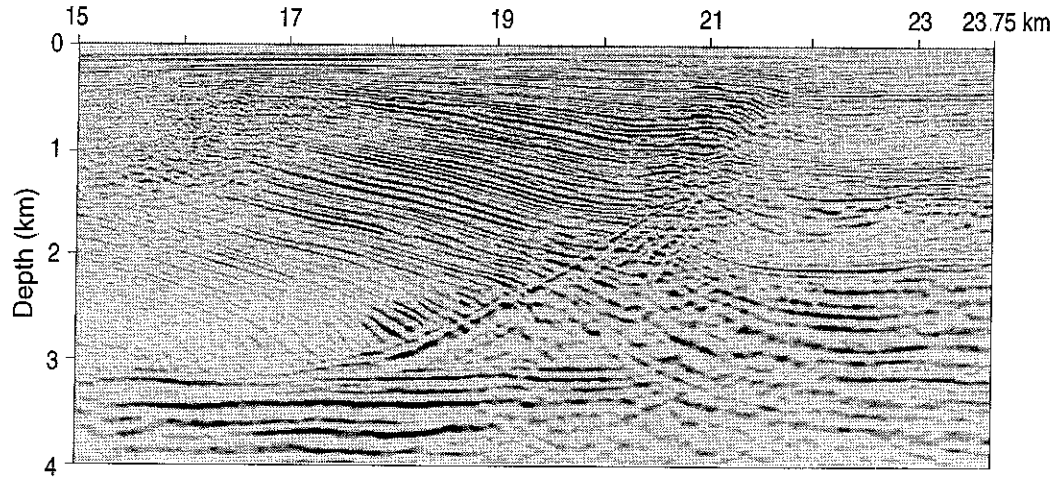

Figure 13. Post-migration stacked section associated with the blocky model in Fig 4.

migration. The smoothing would give ray-traced traveltimes that have nothing to do with those associated with the original blocky model.

We examine below the practicality of migration velocity analysis, i.e. of interpretation of the cube of common-offset depth-migrated images, when a blocky or a smooth model is used for migration. To avoid the above-mentioned difficulties associated with the use of Kirchhoff migration on blocky models, we use the common-offset wave-field migration algorithm of Ehinger, Lailly & Marfurt (1994). Such an algorithm is robust with respect to perturbations of interface geometries.

The goal of depth migration is to put reflections in their correct places and to join reflections which split during propagation in a medium with lateral velocity discontinuities. This said, we immediately realize some difficulties when migration velocity analysis is performed with an erroneous blocky velocity model. Instead of joining reflections, we will, in general (since the velocity discontinuities are misplaced), do the opposite, and further split these reflections. Migration velocity analysis then appears to be very difficult, or even impossible (Fig. 14), as interpretation of events relies mainly on their continuity. In contrast, a smooth velocity model, even if erroneous, preserves the continuity of seismic events during the migration process (Fig. 15). Migration velocity analysis can then be effective.

5 CONCLUSIONS

Seismic imaging of geological structures with severe lateral velocity variations calls for the use of adequate imaging techniques, such as pre-stack depth migration, and for accurate determination of the distribution of propagation velocities. Reflection tomography and migration velocity analysis are attractive techniques for this determination. Two kinds of subsurface representations are classically used in this context: blocky models and smooth models.

We have seen some difficulties associated with the use of blocky models: they can result in non-convergence of the reflection tomography iterative process; and when the model is erroneous, the interpretation of individual common-offset images, which is the basis of migration velocity analysis, can be extremely difficult.

Although smooth models do not offer perfect kinematic consistency with the seismic data associated with such complex geological structures, they have the potential, through an

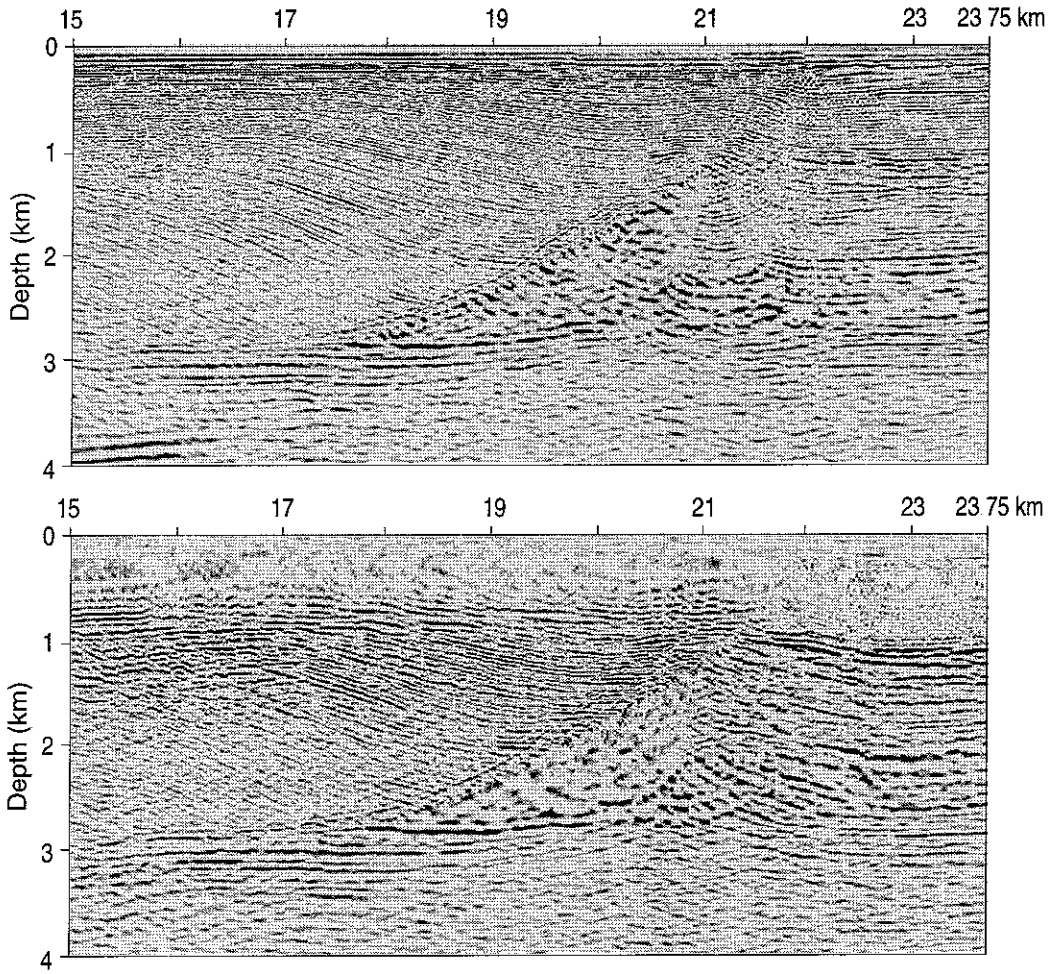

Figure 14 Common-offset migrated sections associated with the blocky model in Fig. 4. Results are for offsets of 200 m (top) and 1500 m (bottom). For migration velocity analysis, we are interested in the images of deep events, such as the base of the salt, for surface locations ranging between 20 and 22 km. The discontinuities of these events and the many interferences make their picking very difficult, if not impossible.

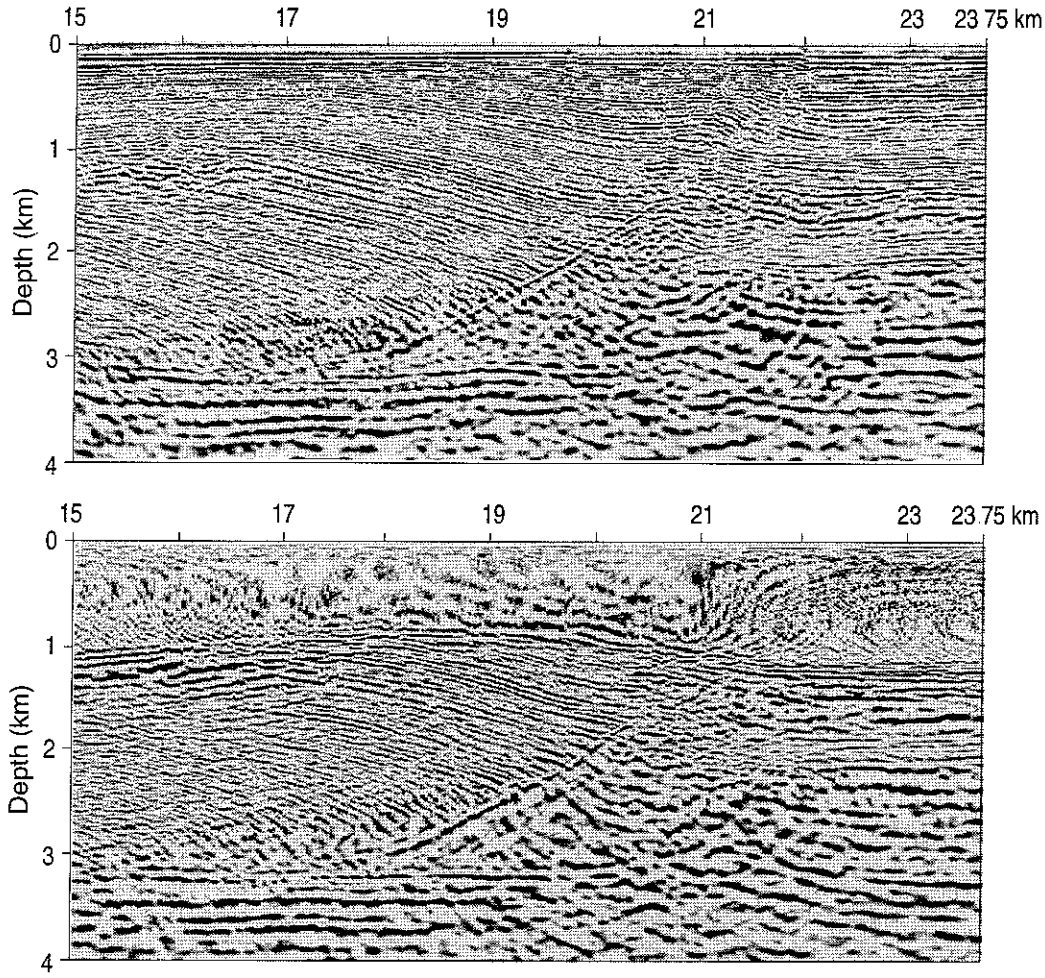

Figure 15. Common-offset migrated section associated with the smooth model in Fig 8 Top: result for an offset of 200 m Since the migration has been performed with an erroneous velocity model, the events have to be understood as deformed images of the actual geological structure To perform migration velocity analysis, we are interested in the identification of events for which we have no traveltime data, for instance the reflection on the base of the salt or deeper events Knowing that the basement consists of flat, parallel layers, we can easily identify such events, which are split into three pieces: the left piece is nearly horizontal and situated between surface locations 15 and 20 km; the right piece, horizontal at the right edge, is progressively pulled up when moving from surface location 22 km to surface location 21 km; and the central piece is almost circular for surface locations ranging between 21 and 22 km Bottom: result for an offset of 1500 m The same comments as in the top diagram apply, but the central piece of the migrated events has disappeared whereas the left piece goes further to the right and is then strongly pulled up.

approximate kinematic consistency, to give reasonable seismic images of such structures.

Reflection tomography and migration velocity analysis are appropriate techniques to complete this approximate kinematic consistency. Smooth models are then quite suited to run such techniques: together with an adequate integration of *a priori* geological information, they provide us with a reliable reflection tomography avoiding possible local minima; and they make possible the difficult interpretation of the cube of common-offset migrated images, which is the key for migration velocity analysis

ACKNOWLEDGMENTS

This research was carried out as part of the Prestack Structural Interpretation consortium project (PSI) The authors hereby acknowledge the support provided by the sponsors of this project. One of the authors (DS) wishes to thank Elf Aquitaine for its financial support. We acknowledge TOTAL, who provided the real data set studied in this paper and we thank the members of the PSI team, especially Andreas Ehinger for his invaluable cooperation We also thank several scientists from the Amoco Research Center who have inspired various aspects of this paper: Larry Lines and John Scales for the very instructive discussions we have had about reflection tomography; Sam Gray who put a lot of effort into pushing us towards the common-offset strategy, which is the adequate one for migration velocity analysis; Kurt Marfurt, with whom we have cooperated on many subjects, especially on the development of the common-offset migration program used to produce some of the results presented in this paper; and especially Sven Treitel, who was the initiator of the many fruitful exchanges we have had with Amoco for more than 15 years.

REFERENCES

Apostoiu-Marin, I & Ehinger A, 1994 Kinematical exercises on prestack depth migrated images, *Geophysics* submitted.

Barsky, R.H., Bartels, B.A. & Beatty, J.C., 1986. *An introduction to splines for use in computer graphics and geometry modeling.* Morgan Kaufmann Publishers, Los Altos.

Bishop, T.N., Bube, K.P., Cutler, R.T., Love, P.L., Resnick, J.R., Shuey, R.T., Spindler, D.A. & Wyld, H.W., 1985. Tomographic determination of velocity and depth in laterally varying media, *Geophysics*, **50,** 903–923.

Bording, R.P., Gersztenkorn, A., Lines, L., Scales, J.A. & Treitel, S., 1987. Applications of seismic travel-time tomography, *Geophys. J. R. astr. Soc.*, **90,** 285–303.

Chiu, S.K.L. & Stewart, R.R., 1987. Tomographic determination of three-demensional seismic velocity structure using well logs, vertical seismic profiles, and surface seismic data, *Geophysics*, **52,** 1085–1098.

de Bazelaire, E. & Viallix, J.R., 1988. Optical interpretation of seismic events, part II: distorted NMO curves can tell where to drill, paper presented at *50th Mtg. Eur. Assn. Expl. Geophys.* The Hague.

Delprat-Jannaud, F. & Lailly, P., 1993. Ill-posed and well-posed formulations of the reflection tomography problem, *J. geophys. Res.*, **98,** 6589–6605.

Delprat-Jannaud, F. & Lailly, P., 1995. Reflection tomography: how to handle multiple arrivals?, *J. geophys. Res.*, **100,** 703–715.

Delprat-Jannaud, F., Farra, V., Jardin, A., Jacobs, J.A.C., Lailly, P. & Versteeg, R., 1991. A first application of the PSI approach on 2D data, *PSI 1991 Annual Report.* Institut Français du Pétrole, Rueil-Malmaison, France.

Ehinger, A., Lailly, P. & Marfurt, K., 1994. Green's function implementation of commom offset wave equation migration, *Geophysics*, submitted.

Geoltrain, S. & Brac, J., 1993. Can we image complex structures with first-arrival traveltime?, *Geophysics*, **58,** 564–575.

Glowinski, R. & Tran, Q.H., 1993. Constrained optimization in reflection tomography, the Augmented Lagrangian method: East-West, *J. Numer. Math.*, **1,** 213–234.

Harlan, W.S., 1992. Robust strategies for reflection and crosswell traveltime tomography, *54th Mtg. Eur. Assn. Expl. Geophys.* Expanded Abstracts, 250–251.

Jacobs, J.A.C., Delprat-Jannaud, F., Ehinger, A. & Lailly, P., 1992. Sequential migration-aided reflection tomography: A tool for imaging complex structures, *63rd Ann. Internat. Mtg. Soc. Expl. Geophys.* Expanded Abstracts, 231–234.

Jannaud, L. & Delprat-Jannaud, F., 1995. Traveltime inversion with *a priori* information on illuminated parts of the reflectors, *J. Geophys. Res.*, **100,** 2151–2160.

Lailly, P. & Ehinger, A., 1991. Overview of the PSI approach to complex structure imaging, *PSI 1991 Annual Report.* Institut Français du Pétrole, Rueil-Malmaison, France.

Lines, L.R. & Treitel, S., 1985. Inversion with a grain of salt, *Geophysics*, **50,** 99–109.

May, B.T. & Covey, J.D., 1983. Structural inversion of salt dome flanks, *Geophysics*, **48,** 1039–1050.

Sinoquet, D., 1993. Modeling *a priori* information on velocity field in reflection tomography, *63rd Ann. Internat. Mtg. Soc. Expl. Geophys.* Expanded Abstracts, 591–594.

Stork, C., 1992. Reflection tomography in the postmigrated domain, *Geophysics*, **57,** 680–692.

van Trier, J., 1990. Structural velocity analysis, *PhD thesis.* Stanford University, Palo Alto.

Versteeg, R.J., 1991. Analyse du problème de la détermination du modèle de vitesse pour l'imagerie sismique, *PhD thesis.* Université Paris VII, France.

Wang, S.S., Baumel, R.T., Hanson, D.W., Bell, D.W., Boyd, M., Cavanaugh, T.D., Cox, V.D., D'Onfro, P.S., Durrani, J.A. & Standlee, L.A., 1991. *Common offset depth migration as a velocity analysis tool. the Marmousi Experience.* Eur. Assn. Expl. Geophys., Zeist.

Whiting, P.M., 1991. Practical reflection tomography and maximum entropy imaging, *61st Ann. Internat. Mtg. Soc. Expl. Geophys.* Expanded Abstracts, 986–989.

Williams, R.G. & Cowley, J., 1993. Residual depth moveout after common offset depth migration, *55th Mtg. Eur. Assn. Expl. Geophys.* Expanded Abstracts.

Williams, R.G., Cowley, J. & Notfors, C., 1992. Migration velocity analysis using common offset depth migration, *54th Mtg. Eur. Assn. Expl. Geophys.* Expanded Abstracts, 258–259.